


Communication

Generation of High-Quality Cylindrical Vector Beams from All-Few-Mode Fiber Laser

Pingping Xiao ¹, Zhen Tang ², Fei Wang ¹, Yaqiong Lu ² and Zuxing Zhang ^{2,*} 

¹ Department of Electronic Information Engineering, College of Physics and Engineering Technology, Yichun University, Yichun 336000, China; xpp7967@163.com (P.X.)

² College of Electronic and Optical Engineering, Nanjing University of Posts and Telecommunications, Nanjing 210023, China

* Correspondence: zxzhang@njupt.edu.cn

Abstract: Transverse mode control of laser intracavity oscillation is crucial for generating high-purity cylindrical vector beams (CVBs). We utilized the mode conversion and mode selection properties of two-mode long-period fiber gratings (TM-LPFGs) and two-mode fiber Bragg gratings (TM-FBGs) to achieve intracavity hybrid-mode oscillations of LP₀₁ and LP₁₁ from an all-few-mode fiber laser. A mode-locked pulse output with a repetition rate of 12.46 MHz and a signal-to-noise ratio of 53 dB was achieved with a semiconductor saturable absorber mirror (SESAM) for mode-locking, at a wavelength of 1550.32 nm. The 30 dB spectrum bandwidth of the mode-locked pulse was 0.13 nm. Furthermore, a high-purity CVB containing radially polarized and azimuthally polarized LP₁₁ modes was generated. The purity of the obtained CVB was greater than 99%. The high-purity CVB pulses have great potential for applications in optical tweezers, high-speed mode-division multiplexing communication, and more.

Keywords: cylindrical vector beams; few-mode fiber; two-mode fiber Bragg grating; mode-locked pulse



Citation: Xiao, P.; Tang, Z.; Wang, F.; Lu, Y.; Zhang, Z. Generation of High-Quality Cylindrical Vector Beams from All-Few-Mode Fiber Laser. *Photonics* **2024**, *11*, 975. <https://doi.org/10.3390/photonics11100975>

Received: 12 September 2024

Revised: 5 October 2024

Accepted: 14 October 2024

Published: 17 October 2024



Copyright: © 2024 by the authors. Licensee MDPI, Basel, Switzerland. This article is an open access article distributed under the terms and conditions of the Creative Commons Attribution (CC BY) license (<https://creativecommons.org/licenses/by/4.0/>).

1. Introduction

Cylindrical vector beams (CVBs) with polarization singularities have important applications in laser material processing [1,2], particle trapping [3,4], and various other fields. The mode purity of CVBs plays a crucial role in enhancing the efficiency of material processing and improving the precision of optical tweezers [5]. Meanwhile, the rapidly developing information technology increasingly demands larger communication capacities. The efficient utilization of optical spectrum resources is a crucial prerequisite for improving channel capacity. Beam parameter management enables the parallel transmission of multi-channel information, greatly improving the transmission capacity of optical communication systems [6]. Among these, mode-division multiplexing (MDM) technology [7,8], which involves transmitting multiple modes through few-mode fibers or multi-mode fibers, has received increasing attention. High-order mode fiber lasers have opened up potential applications in large communication capacity systems due to their unique polarization and spatial intensity distribution characteristics. For example, the orbital angular momentum (OAM) beam [9,10] is a special light field with a continuous helical phase wavefront.

In recent years, research on the generation of CVBs in optical fibers has garnered extensive attention. All-fiber mode-selection couplers (MSCs) with dual-port outputs [11,12], few-mode long-period fiber gratings (FM-LPFGs) with high conversion efficiency [13,14], simple dislocation splicing methods [15,16], and dynamically tuned acoustic-induced fiber gratings (AIFGs) [17,18] have been used to obtain both radial and azimuthal vector beams. The realization of ultrashort pulsed vector beams from fiber lasers using these methods has also been extensively investigated. In 2017, a passive mode-locked laser with an MSC inserted into a figure-of-eight cavity was demonstrated [19], achieving a CVB output with a purity greater than 94%. In 2021, an ultra-wideband LPFG mode converter with a flat

conversion bandwidth was fabricated, which produced CVB-dissipative solitons with a purity greater than 96% [20]. Zhan et al. used single-mode fiber and four-mode fiber offset splicing to obtain a CVB pulse output with a purity of 97.14% [21]. However, all of the lasers that generate ultrashort pulse CVB are based on the oscillation of the fundamental mode in the cavity, and the mode conversion purity is limited by the operation of the fundamental mode in the cavity.

All-few-mode fiber lasers provide a new approach for generating high-quality CVBs. Compared with traditional fundamental-mode oscillation fiber lasers, it is intriguing to investigate the transverse mode competition and the intracavity dynamics in all-few-mode cavities. In 2019, Wang et al. reported a Q-switched all-few-mode ring fiber laser cavity, where higher-order mode oscillation in the cavity generated optical vortex beams (OVBS) with a purity of 96% [22]. Subsequently, Lv et al. reported a laterally mode-switchable mode-locked fiber laser with a few-mode fiber linear cavity, which achieved switchable oscillations of the laser in both the fundamental and higher-order modes, and obtained a CVB with a purity of 98.6% [23]. However, there are few reports on hybrid-mode oscillation in all-few-mode fiber lasers.

In this paper, we construct an all-few-mode ring fiber laser cavity and achieve hybrid-mode oscillation through the integration of few-mode gratings. Based on a semiconductor saturable absorber mirror (SESAM), mode-locking in the cavity was achieved, resulting in narrow-band CVB mode-locked pulses with a wavelength of 1550.32 nm and a 30 dB bandwidth of 0.13 nm. The mode purity of radially polarized light (RPL) and azimuthally polarized light (APL) of the CVB mode-locked pulses measured at the output were 99.2% and 99.4%, respectively. The study of hybrid-mode oscillation in all-few-mode cavities plays an important role in promoting the acquisition of high-quality CVB pulses.

2. Characteristics of Fiber Gratings

A TM-LPFG was used as a mode converter in the cavity. It was inscribed on a two-mode fiber (TMF) (OFS, two-mode step index fiber, 19/125 μm), which can achieve mode conversion between the LP_{01} mode and the LP_{11} mode with high efficiency. This means that not only can the LP_{01} mode be converted to the LP_{11} mode, but the LP_{11} mode can also be converted to the LP_{01} mode. To obtain the conversion efficiency from LP_{01} mode to LP_{11} mode, we measured the transmission spectrum of the TM-LPFG. The broadband source was emitted into the TM-LPFG, and the single-mode fiber (SMF) connected to both sides of the TM-LPFG was bent to a radius of less than 2 cm to attenuate higher-order modes, ensuring that only the LP_{01} mode was detected by the optical spectrum analyzer (OSA) at the output. The measured loss peak corresponds to the conversion from LP_{01} mode to LP_{11} mode, as shown in Figure 1. This loss peak reflects the mode conversion efficiency of the TM-LPFG. As can be seen from Figure 1, the mode conversion efficiency of the TM-LPFG is greater than 90% (10 dB) in the bandwidth range of 27 nm (1531–1558 nm), and the peak efficiency is greater than 99% (20 dB).

The TM-FBG is also inscribed on the same TMF (OFS, two-mode step index fiber, 19/125 μm) as a mode selector. We measured the reflection spectra of the TM-FBG under different injection modes, as illustrated in Figure 2. The black curve in Figure 2 represents the measurement results when only the LP_{01} mode is incident on the fiber. A distinct reflection peak at 1551.64 nm is observed, corresponding to the self-coupling of the LP_{01} mode. Subsequently, we examined the reflection spectrum of the TM-FBG with the LP_{11} mode injection, where the higher-order mode is excited through the TM-LPFG. This is shown by the red curve in Figure 2. The left peak at 1550.3 nm corresponds to the self-coupling of the LP_{11} mode, while the right peak at 1550.94 nm corresponds to the mutual coupling of the LP_{01} and LP_{11} modes. Notably, there is no self-coupling spectrum observed for the LP_{01} mode, which indirectly indicates that the TM-LPFG can convert almost all of the fundamental modes to higher-order modes. The combination of the TM-FBG and the TM-LPFG can be perfectly integrated into an all few-mode fiber laser, and the presence

of the intracavity oscillation mode can be inferred by observing the transmission of the TM-FBG.

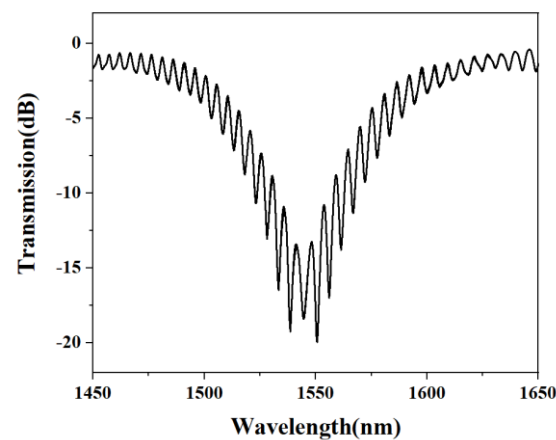


Figure 1. TM-LPFG transmission spectrum.

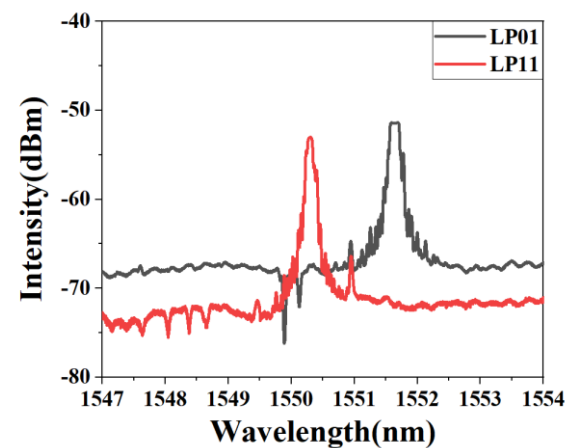


Figure 2. TM-LPFG transmission spectra under different injection modes (black curve for LP₀₁ injection; red curve for LP₁₁ injection).

3. Experimental Setup and Results

A schematic diagram of the all-few-mode fiber laser based on few-mode fiber gratings is shown in Figure 3. The 976 nm LP₁₁ mode pump light is injected into the 4 m few-mode erbium-doped fiber (FM-EDF) (19/125 μm , NA = 0.6) through a hand-made wavelength division-multiplexing mode-selection coupler (WDM-MS). The unidirectional transmission of the ring cavity is ensured by using a few-mode fiber circulator (FM-Cir). The TM-LPFG and the TM-FBG are connected to port 2 of the FM-Cir 1 in sequence. A home-made 90:10 few-mode fiber (FMF) optical coupler was used to observe the output of the laser cavity. The SESAM used for mode-locking was placed in the middle of the two few-mode connectors and was connected to the laser cavity through the FM-Circ 2. A polarization controller (PC1) was utilized to flexibly switch the polarization states and obtain stable mode-locked pulses. All components in the laser cavity were connected by FMFs (OFS, two-mode step index fiber, 19/125 μm). The output spectrum and pulse train of the laser are measured at output 1 using an optical spectrum analyzer (OSA, Yokogawa AQ6370D) and an oscilloscope (OSC, RIGOL-DS4054), respectively. The output beam profiles at output 1 and output 2 are monitored using a CCD camera (CinCam IR) after passing through a collimator.

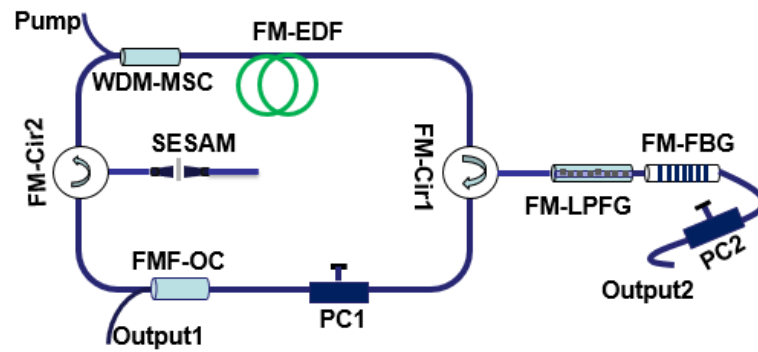


Figure 3. Schematic diagram of the all-few-mode fiber laser.

When the pump power is greater than 640 mW, stable mode-locked pulses are obtained by adjusting polarization controller 1 (PC1). The output spectrum and pulse sequence from output 1 at a pump power of 700 mW are shown in Figure 4a,b, respectively. The working wavelength of the narrow linewidth fiber laser is 1550.32 nm with a 30 dB spectrum width of 0.13 nm. The pulse period was found to be 80.5 ns by measuring the interval between adjacent pulses.

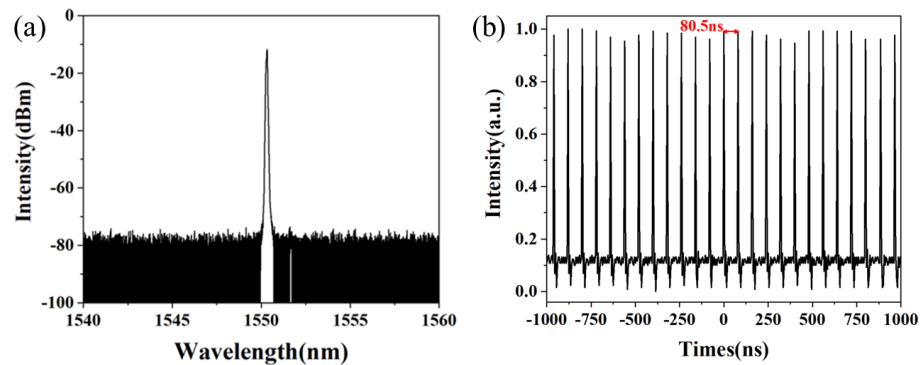


Figure 4. (a) Output spectrum and (b) pulse train of the laser.

Figure 5a depicts the radio frequency (RF) spectrum of the mode-locked pulses. The signal-to-noise ratio is 53 dB and the repetition rate is 12.46 MHz. The calculated cavity length from the measured repetition rate is approximately 16 m, which is consistent with the actual cavity length. Figure 5b shows the RF spectrum in the range of 2 GHz. It can be seen that the mode-locked laser is in a stable state.

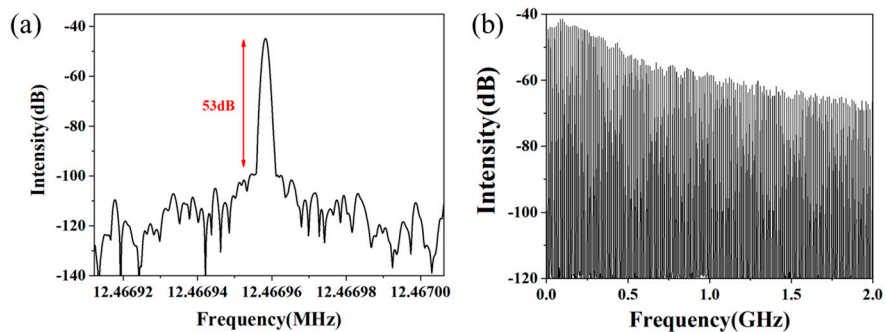


Figure 5. Radio frequency spectra of mode-locked pulse train in the range of: (a) 0.1 KHz and (b) 2 GHz.

Figure 6 shows the relationship between the output power from the two output ports and the pump power. It can be seen that the output power from the two output ports maintains a linear relationship with the pump power. The slope efficiencies of the output

power from output 1 and output 2 are 1.23% and 3.11%, respectively. The slope efficiency of the laser is relatively low because some devices in the laser are made by us, which will cause certain losses.

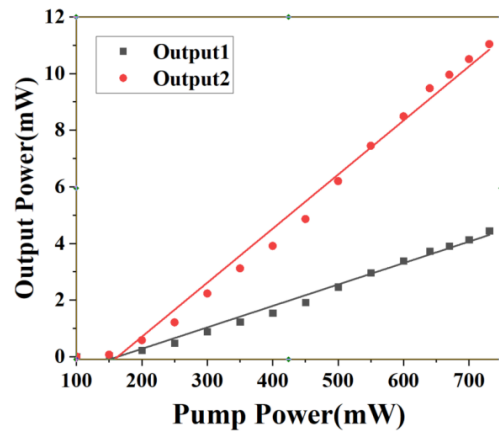


Figure 6. The relationship between output power and pump power for two outputs.

By adjusting PC2, a CVB with doughnut-shaped intensity distribution, as shown in Figure 7a,f, can be observed with the CCD camera. RPL and APL can be distinguished by rotating the polarizer placed between the collimator and the CCD camera. The mode field intensity distributions of RPL and APL are shown in Figures 7b–e and 7g–j, respectively, and the mode purity is measured to be 99.2% and 99.4%, respectively, by using the bending method.

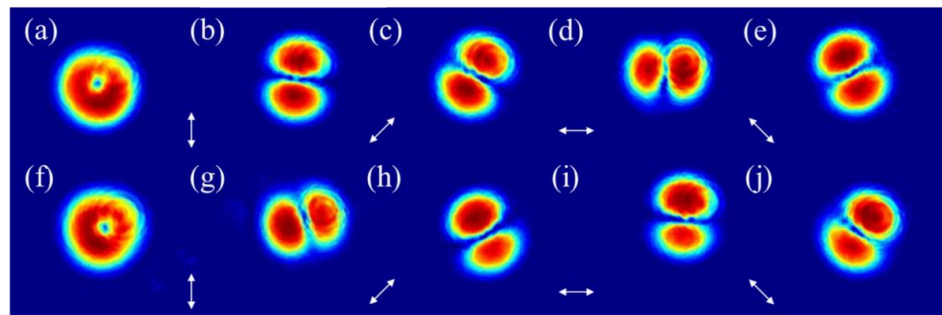


Figure 7. Optical intensity distribution monitored at output 1: (a–e) RPL and (f–j) APL.

From the above observation, it can be seen that the all few-mode fiber lasers can realize the output of CVB pulses, but the mode of intracavity oscillation still cannot be determined. Now, we will discuss the mode of intracavity oscillation of the laser from the perspective of output mode and output spectrum.

First, we analyze the output mode: the intensity distribution from output 2 measured by the CCD camera, when mode locking was observed, is shown in Figure 8a. By observing the shape of the beam, we infer that it is not a pure fundamental mode but a mixed mode of LP_{01} and LP_{11} . The beam shape is slightly elliptical rather than a perfect circle. Then, by reducing the pump power (600 mW) and without changing other conditions, we can obtain the beam intensity distribution in a certain polarization state as shown in Figure 8b, exhibiting a mode field distribution that more closely resembles the shape of higher-order modes. This suggests that the TM-FBG reflects the mixed mode. In addition, the mixed mode does not affect the mode conversion of the TM-LPFG. Through the mode conversion of the TM-LPFG, LP_{01} is converted to LP_{11} , and LP_{11} is converted to LP_{01} . Therefore, the intracavity oscillation mode is a mixed mode.

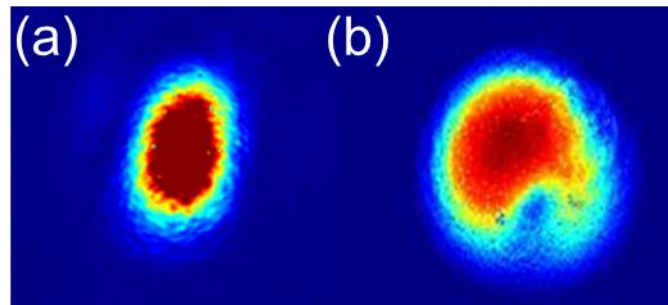


Figure 8. Light field distribution measured at output 2 under different pump power: (a) 700 mW, (b) 600 mW.

Then, we can analyze the output mode from the perspective of the spectrum: the output spectra of output 1 (black curve) and output 2 (red curve) under mode locking are shown in Figure 9. This Figure shows that both the output 1 and output 2 spectra have small reflection and transmission peaks at 1551.63 nm. This wavelength corresponds to the self-coupling peak of LP₀₁ mode in the TM-FBG, which means that the light reflected back into the cavity contains a small proportion of LP₀₁ mode and a large proportion of LP₁₁ mode. After the TM-LPFG, the LP₁₁ mode and LP₀₁ mode oscillate in the laser at the same time, so the oscillation mode of the mode-locked laser is mixed mode.

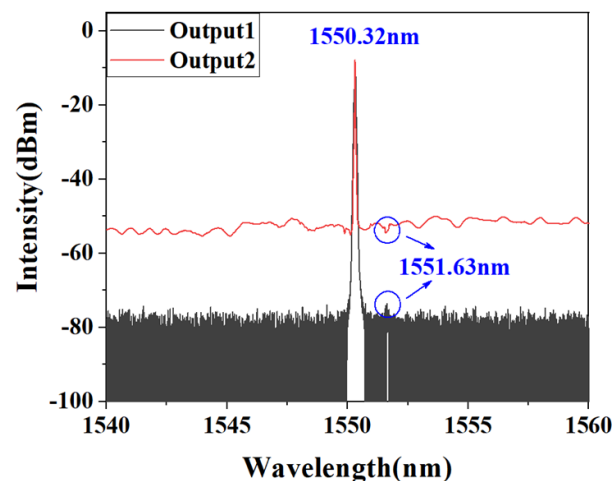


Figure 9. Output spectra of the mode-locked laser from output 1 and output 2 at the same time.

In addition, since TMF-OC can perform mode conversion at a coupling ratio of 90:10 [12], this means that the high-order mode output at the output 1 end may be converted into a high-order mode due to its own characteristics, and may not necessarily be the mode of intracavity oscillation. Replacing the 90:10 TMF-OC with a 60:40 TMF-OC (without mode conversion function) allows us to measure and analyze the output of the all few-mode fiber laser in CW state, and verify the intracavity oscillation mode. The intensity distribution of the light spots of output 1 and output 2 was observed using a CCD camera. It can be seen that the light spot at output 1 is a high-order mode and the light spot at output 2 is a mixed mode. However, it should be noted that both light spots only have one polarization direction as a high-order mode, and they exhibit irregular elliptical shapes in other polarization states. The shape of the light spots is similar to Figure 8a, which also proves that the oscillation mode in the cavity under CW state is a mixed mode.

4. Conclusions

In summary, we have achieved a cylindrical vector beam output with a purity greater than 99% through hybrid-mode oscillation in an all-few-mode fiber laser. The pump light source is converted into higher-order modes and injected into the cavity. The LP₀₁

and LP₁₁ mixed modes are excited in the laser cavity utilizing the combined properties of TM-LPFG and TM-FBG. A narrow-band cylindrical vector mode-locked pulse with a wavelength of 1550.32 nm, a 30 dB bandwidth of 0.13 nm, and a pulse period of 80.5 ns is generated. We believe that high-purity cylindrical vector beams are of great significance to the development of material processing, particle trapping, optical communications, and other advanced applications.

Author Contributions: Conceptualization, Z.Z. and P.X.; methodology, P.X.; software, P.X.; validation, P.X., Z.T. and F.W.; formal analysis, P.X.; investigation, P.X.; resources, Z.Z.; data curation, P.X.; writing—original draft preparation, P.X. and Z.T.; writing—review and editing, P.X., Z.T., Y.L. and Z.Z.; visualization, P.X.; supervision, Z.Z.; project administration, Z.Z.; funding acquisition, Z.Z. All authors have read and agreed to the published version of the manuscript.

Funding: This work was supported by the National Natural Science Foundation of China (Grant No.11664043, No.81660105, No.11764020), and the Science & Technology Project of Department of Education of Jiangxi Province (Grant No. GJJ2401601).

Institutional Review Board Statement: Not applicable.

Informed Consent Statement: Not applicable.

Data Availability Statement: Data are contained within the article.

Conflicts of Interest: The authors declare no conflicts of interest.

References

- Phillips, K.C.; Gandhi, H.H.; Mazur, E.; Sundaram, S.K. Ultrafast laser processing of materials: A review. *Adv. Opt. Photonics* **2015**, *7*, 684–712. [[CrossRef](#)]
- Kozawa, Y.; Sato, M.; Uesugi, Y.; Sato, S. Laser microprocessing of metal surfaces using a tightly focused radially polarized beam. *Opt. Lett.* **2020**, *45*, 6234–6237. [[CrossRef](#)]
- Huang, L.; Guo, H.; Li, J.; Ling, L.; Feng, B.; Li, Z.Y. Optical trapping of gold nanoparticles by cylindrical vector beam. *Opt. Lett.* **2012**, *37*, 1694–1696. [[CrossRef](#)]
- Min, C.; Shen, Z.; Shen, J.; Zhang, Y.; Fang, H.; Yuan, G.; Du, L.; Zhu, S.; Lei, T.; Yuan, X. Focused plasmonic trapping of metallic particles. *Nat. Commun.* **2013**, *4*, 2891. [[CrossRef](#)]
- Padgett, M.; Bowman, R. Tweezers with a twist. *Nat. Photonics* **2011**, *5*, 343–348. [[CrossRef](#)]
- Klaus, W.; Puttnam, B.J.; Luis, R.S.; Sakaguchi, J.; Mengueta JM, D.; Awaji, Y.; Wada, N. Advanced space division multiplexing technologies for optical networks. *J. Opt. Commun. Netw.* **2017**, *9*, C1–C11. [[CrossRef](#)]
- Puttnam, B.J.; Rademacher, G.; Luis, R.S. Space-division multiplexing for optical fiber communications. *Optica* **2021**, *8*, 1186–1203. [[CrossRef](#)]
- Weerdenburg, J.V.; Ryf, R.; Alvarado-Zacarias, J.C.; Alvarez-Aguirre, R.A.; Fontaine, N.K.; Chen, H.; Correa, R.A.; Sun, Y.; Gruner-Nielsen, L.; Jensen, R. 138 Tbit/s mode- and wavelength multiplexed transmission over 6-mode graded-index fiber. *J. Light. Technol.* **2018**, *36*, 1369–1374. [[CrossRef](#)]
- Wang, A.; Zhu, L.; Wang, L.; Ai, J.; Chen, S.; Wang, J. Directly using 8.8-km conventional multi-mode fiber for 6-mode orbital angular momentum multiplexing transmission. *Opt. Exp.* **2018**, *26*, 10038–10047. [[CrossRef](#)]
- Ramachandran, S.; Gregg, P.; Kristensen, P.; Golowich, S.E. On the scalability of ring fiber designs for OAM multiplexing. *Opt. Exp.* **2015**, *23*, 3721–3730. [[CrossRef](#)]
- Ismaeel, R.; Lee, T.; Oduro, B.; Jung, Y.; Brambilla, G. All-fiber fused directional coupler for highly efficient spatial mode conversion. *Opt. Exp.* **2014**, *22*, 11610–11619. [[CrossRef](#)]
- Xu, Y.; Chen, S.; Wang, Z.; Sun, B.; Wan, H.; Zhang, Z. Cylindrical vector beam fiber laser with a symmetric two-mode fiber coupler. *Photonics Res.* **2019**, *7*, 1479–1484. [[CrossRef](#)]
- Zhao, Y.; Liu, Y.; Zhang, L.; Zhang, C.; Wen, J.; Wang, T. Mode converter based on the long-period fiber gratings written in the two-mode fiber. *Opt. Exp.* **2016**, *24*, 6186–6195. [[CrossRef](#)]
- Yang, C.; Zhang, C.; Fu, S.; Shen, L.; Wang, Y.; Qin, Y. Mode converter with C+L band coverage based on the femtosecond laser inscribed long period fiber grating. *Opt. Lett.* **2021**, *46*, 3340–3343. [[CrossRef](#)]
- Grosjean, T.; Courjon, D.; Spajer, M. An all-fiber device for generating radially and other polarized light beams. *Opt. Commun.* **2002**, *203*, 1–5. [[CrossRef](#)]
- Mao, D.; Feng, T.; Zhang, W.; Lu, H.; Jiang, Y.; Li, P.; Jiang, B.; Sun, Z.; Zhao, J. Ultrafast all-fiber based cylindrical-vector beam laser. *Appl. Phys. Lett.* **2017**, *110*, 021107. [[CrossRef](#)]
- Song, D.R.; Su Park, H.; Kim, B.Y.; Song, K.Y. Acoustooptic generation and characterization of the higher order modes in a four-mode fiber for mode-division multiplexed transmission. *J. Light. Technol.* **2014**, *32*, 3932–3936.
- Kim, B.Y.; Blake, J.N.; Engan, H.E.; Shaw, H.J. All-fiber acousto-optic frequency shifter. *Opt. Lett.* **1986**, *11*, 389–391. [[CrossRef](#)]

19. Wan, H.; Wang, J.; Zhang, Z.; Cai, Y.; Sun, B.; Zhang, L. High efficiency mode-locked, cylindrical vector beam fiber laser based on a mode selective coupler. *Opt. Exp.* **2017**, *25*, 11444–11451. [[CrossRef](#)]
20. Feng, M.; He, J.; Mao, B.; Cheng, W.; Wang, P.; Wang, Z.; Yue, Y.; Liu, Y. Generation of cylindrical vector dissipative soliton using an ultra-broadband LPFG mode converter with flat conversion efficiency. *Opt. Exp.* **2021**, *29*, 41496–41511. [[CrossRef](#)]
21. Zhou, Y.; Wang, A.; Gu, C.; Sun, B.; Xu, L.; Li, F.; Chung, D.; Zhan, Q. Actively mode-locked all fiber laser with cylindrical vector beam output. *Opt. Lett.* **2016**, *41*, 548–550. [[CrossRef](#)]
22. Wang, T.; Yang, A.; Shi, F.; Huang, Y.; Wen, J.; Zeng, X. High-order mode lasing in all-FMF laser cavities. *Photonics Res.* **2019**, *7*, 42–49. [[CrossRef](#)]
23. Lv, J.; Dai, C.; Li, H.; Ma, X.; Lin, J.; Gu, C.; Yao, P.; Xu, L.; Zhan, Q. High-efficiency mode-locked fiber laser with a switchable oscillating transverse mode in an all few-mode fiber linear cavity. *Opt. Exp.* **2022**, *30*, 1641–1650. [[CrossRef](#)]

Disclaimer/Publisher’s Note: The statements, opinions and data contained in all publications are solely those of the individual author(s) and contributor(s) and not of MDPI and/or the editor(s). MDPI and/or the editor(s) disclaim responsibility for any injury to people or property resulting from any ideas, methods, instructions or products referred to in the content.